

A comparison of image quality between digital and analog pet for spatial resolution: A phantom study

M.C. Karaca^{1*}, M. Doyuran¹, T. Çakır², S. Karyavaşar³, M. Çağlar¹

¹Department of Health Physics, Graduate School of Health Sciences, İstanbul Medipol University, İstanbul, Türkiye

²Department of Nuclear Medicine, School of Medicine, İstanbul Medipol University, İstanbul, Türkiye

³Department of Nuclear Medicine, Health Science University, Medical Faculty, Prof Dr Cemil Taşçıoğlu City Hospital, İstanbul, Türkiye

ABSTRACT

► Original article

*Corresponding author:

Merve Cinoglu Karaca, M.Sc.,

E-mail:

mervecinoglu@gmail.com

Received: July 2023

Final revised: June 2024

Accepted: July 2024

Int. J. Radiat. Res., April 2025;
23(2): 397-405

DOI: 10.61186/ijrr.23.2.19

Keywords: Digital PET, analog PET, lesion detection capability, image quality.

Background: The positron emission tomography (PET) technology has undergone continuous innovation in recent years. New-technology digital PETs are silicon photomultiplier (SiPM) PET systems with digital readouts, which contribute to improved image resolution. This study aimed to compare the image quality of sub-centimeter lesions of NEMA PET phantom images obtained under identical imaging conditions (identical lesion volumes, identical activity and identical scanning time) using dPET, analog PET-1 and analog PET-2 acquired in the clinic. **Materials and Methods:** For image analysis, a standard NEMA IEC body phantom was used. In the present study, the lesion detection performance of all PETs was evaluated in two categories, sub- and over-centimeter size. The imaging durations of this study were 1, 2, 3, and 5 minutes, while the injection doses were 2.33 and 5.33 kBq/ml for the 1/4 and 1/8 background-to-lesion ratios, respectively. For a quantitative assessment of image quality, a circular ROI with activity concentrations (AC_{mean}) and the mean recovery coefficient were calculated for each lesion via the AC_{mean}. **Results:** Our study revealed approximately 15% greater RC_{mean} values for dPET with SiPM technology compared to the analog PET-2 with PMT technology. However, analog PET-1 exhibited a significant lack of performance, especially when compared to analog PET-2 and dPET. **Conclusion:** Although dPET, the first generation of dPETs analyzed in the present study, yields relatively better RC_{mean} values than analog PETs, it is not able to entirely eliminate the unfavorable impacts of PVE for sub-centimeter lesions.

INTRODUCTION

Digital PET (dPET) represents the latest development in the last 60 years of PET technology. The new technology in PET systems uses a silicon photomultiplier (SiPM), which is more advanced than analog PET systems with photon multiplier tubes (PMTs). Electron multiplication of the analog PET technology involves an anode-cathode array (dynode) with a potential difference of approximately 100 volts. During their application, photocathode electrons intensify at a factor of 10^6 - 10^7 and reach a level where they can be processed electronically ⁽¹⁾. However, PMTs have several limitations in terms of quantum efficiency (especially when the photons of incoming light are converted into electrons), large-volume pack size, relatively high cost, and high sensitivity to magnetic fields ⁽²⁾. In addition, the analog PET detector design includes a large number of scintillation crystals (e.g., 169 pieces) connected to a small number (e.g., four pieces) of PMTs. These problems can cause inaccurate positioning of the lesions, limited spatial resolution in the detector, and undesirable dead time in the detectors ⁽³⁾.

In the dPET technology that has been recently introduced in the clinic, SiPMs are used instead of PMTs for photon reproduction. By using silicon (Si) (p/n), a semiconductor diode in SiPMs, designers have attempted to prevent the abovementioned disadvantages of PMTs. This technology consists of directing scintillation photons created in the detector's crystal (Lutetium Yttrium Silicate Oxyortho-LYSO) straight to the Si semiconductor, and the photon-electron transformation is produced by the Geiger avalanche owing to the tunneling effect with the reverse bias applied to the silicon semiconductor. By eliminating the voltage effect and that of the anode-cathode sequence, this method aims to achieve highly efficient and stable currents. As SiPMs (also called multipixel detectors) can be produced in desired small volumes, lesion positioning can be achieved with increased accuracy ⁽¹⁾.

The reduced Compton scattering of semiconductor detectors compared to that of PET scintillation detectors can also improve the visibility of the lesion. In recent studies, Telluride (CZT) and Thallium Bromide (TlBr) semiconductor technologies have been used as PET detectors ⁽⁴⁻⁶⁾. The advantages

of this approach are as follows: (i) TlBr has a higher stopping power and higher photofraction than *Bismuth germanium oxide* (BGO); (ii) when using the collected charge, TlBr has better energy resolution and the potential for improved spatial resolution (including DOI, which can be determined by pulse shape changes with depth) compared to BGO or L(Y)SO; and (iii) TlBr has the potential to produce Cherenkov light as efficiently as BGO when using the Cherenkov signal.

The dPET technology, created to increase spatial resolution, specifically aims to obtain accurate images of small lesions. This method attempts to overcome the partial volume effect (PVE), one of the long-standing and most important problems in radionuclide imaging. The smaller the diameter of a lesion, the greater the PVE⁽⁷⁾.

The progress in PET technology has not been related to photon replication methods. Reconstruction algorithms are also constantly improved. After iterative reconstruction algorithms became a standard for PETs, algorithms such as time of flight (ToF) correction and point spread function (PSF) modeling were added to the ordered subset expectation maximization (OSEM) algorithm⁽⁸⁻¹⁰⁾. One of the latest advances in the algorithm field is the Bayesian penalized Probability (BPL) algorithm (trade name: Q.Clear), which is a non-OSEM algorithm that was introduced to clinics by General Electric (GE)⁽¹¹⁾. The penalty function serves as a term for suppressing noise and is regulated by a dimensionless penalty factor (beta value)⁽¹²⁾. In this algorithm, the beta value is the only parameter that can be changed; thus, this parameter helps to determine the Q-Clear algorithm's global strength of regularization. The BPL algorithm also includes the ToF algorithm, an iterative reconstruction algorithm. However, this algorithm aims to reduce the noise ratio and increase the visibility of the lesion.

Early diagnosis of cancer is extremely important in treatment strategies. The earlier a malignant lesion is diagnosed, the more successful the treatment tends to be. Early diagnosis of sub-centimeter lesions, particularly in significantly frequent cases such as lymph node metastases (including micrometastases of 0.2-2 mm) in breast cancer, directly affects the treatment strategy and its success⁽¹³⁻¹⁵⁾. Thus, in early diagnosis, PET has become one of the most important tools available for the last 20 years.

Many studies have shown that the technical data of SiPMs are better than those of PMTs^(16, 17). Wagatsuma et al. showed that the sensitivities of SiPM-PET and PMT-PET were 12.62 and 7.50 cps/kBq, respectively⁽¹⁸⁾. A clinical study by Tsutsui et al. involving SiPM-PET and PMT-PET revealed that the average noise equivalent count (NEC) was 17.4 ± 1.72 Mcounts/m in the PMT-PET/CT dataset and $29.1 \pm 2.83 \times 10^6$ counts/m in the SiPM-PET/CT

dataset⁽¹⁹⁾. Although many studies technically compare PMT-PET and SiPM-PET, there are a limited number of studies in the literature comparing the PET performance of these photon multiplication systems using a phantom for sub-centimeter lesions under real clinical conditions.

This study aimed to compare the image quality of sub-centimeter and over-centimeter lesions of PET phantoms imaged under identical imaging conditions, such as identical lesion volumes, identical activity, and identical scanning times for dPET (General Electric (Ge) Digital Discovery MI) and two analog PETs (Philips Gemini TF, Analog PET and Siemens Analog mate PET). In the literature, the number of phantom studies comparing analog-digital PET image quality for sub-centimeter lesions is quite limited. For the first time, the present study conducted measurements using three different PET devices for sub-centimeter lesions, including the new technology dPET, comparing the image quality performances of the devices. Imaging was performed in accordance with NEMA standards using a commercial phantom and a custom-made phantom.

MATERIALS AND METHODS

Phantoms

Phantoms are the most ideal equipment for evaluating the clinical performance of nuclear medicine devices, such as PET and single-photon emission computed tomography (SPECT). Imaging conditions, such as injection dose, duration, etc., can be stably maintained via phantoms, allowing performance comparisons of the devices.

For the image analysis, the study used the standard National Electrical Manufacturers Association (NEMA) IEC Body Phantom™ (Data Spectrum Corp. Durham, NC, USA) according to NEMA Standard Publication No. NU2. The part that represents the phantom background has a volume of 9800 ml. First, new water-filled lesions were fabricated to represent sub-centimeter lesions less than 1 cm in diameter, replacing the original over-centimeter phantom lesions of the phantom. The diameters of the new lesions were 4 mm, 5 mm, 6 mm, 8 mm, and 10 mm, and their volumes were 0.034, 0.065, 0.113, 0.268, and 0.524 cm³, respectively. The wall thickness of the lesions was 1 mm. Second, in addition to sub-centimeter lesion imaging, the original over-centimeter lesions of the phantom were studied. The diameters of the original over-centimeter lesions are 10 mm, 13 mm, 17 mm, 22 mm, 28 mm, and 37 mm in diameter, and their volumes are 0.524, 1.15, 2.57, 5.57, 11.49, and 26.52 cm³, respectively. Figure 1 shows the images of sub-centimeter lesions produced for this study and original over-centimeter lesions of the phantom.

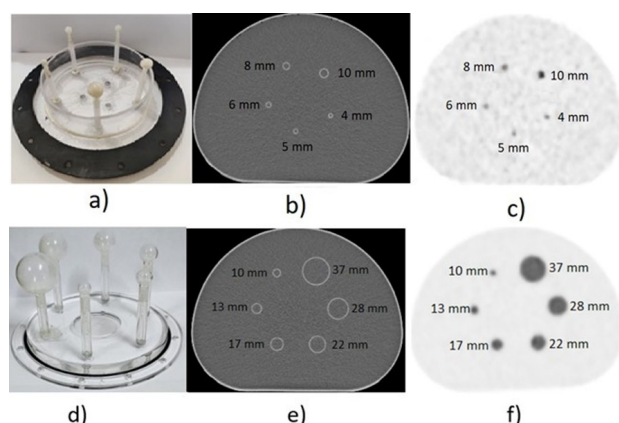


Figure 1. (a) Fabricated sub-centimeter lesions, (b) axial CT images, (c) axial PET images and (d) original over-centimeter lesions, (e) axial CT images and (f) axial PET images.

Positron emission tomography devices

Analog PET-1: This PET uses standard PMT technology. The reconstruction parameters used in this study were three iterations and three subsets, as in the Standard Clinical Protocol (20).

Analog PET-2: Another analog PET used in the study was installed in the clinic in 2021. This PET also uses standard PMT technology. The reconstruction parameters used in this study were two iterations and 21 subsets, as in the Standard Clinical Protocol (21).

dPET: This dPET was installed in the clinic in 2020. This device uses an SiPM with a digital readout. The reconstruction parameters used in the study (Q.Clear Beta value) were Beta=200, as in the Standard Clinical Protocol (22). Table 1 shows some of the technical details of all three devices.

Table 1. Technical parameters of the PETs used in this study (18-20).

Parameter	analog PET-1 [18]	analog PET-2 [19]	digital PET [20]
Installation date	2012	2021	2020
Crystal material	LYSO	LSO	LYSO
Amplifier Type	PMT	PMT	SiPM
Number of rings	3	4	4
Size of crystals [mm ³]	4.0×4.0×22	4×4×20	3.95×5.3×25
Axial FOV [mm]	180	221	200
Bore diameter [mm]	700	780	700
Timing resolution (ps)	600	540	382
Number of CT slice	16	40	128
The CT scan protocol used present study	120 kVp, 100 mAs	120 kVp, 100 mAs	120 kVp, 100 mAs
NEMA Sensitivity [cps/kBq]	7.0	10.0	13.8
Energy Window (keV)	440-665	435-650	425-650
Reconstruction setting used in present study	3 iterations 33 subsets	2 iteration 21 subsets	Beta=200
Matrix size used in present study	144×144	200×200	256×256
Voxel size (mm ³) used in present study	4×4×4	4 ×4 × 3	2.7×2.7×2.8

Image quality measurements and image analysis

One of the performance tests recommended by the NEMA-2012 and NEMA-2018-Reports is image

quality tests. This study used image quality tests following the NEMA recommendations. The PET reconstruction parameters of this study were set as described in the everyday clinical routine (iteration, subset, matrix, beta value, etc. (23,24).

The imaging durations of this study were 1 min, 2 min, 3 min, and 5 min, the durations applicable in clinical practice. NEMA-2012 and NEMA-2018-Reports recommend an injection dose of 5.33 kBq/ml (23,24). However, for some patients, such as those with additional late PET/CT imaging, much lower doses may be applied in the clinic. Consequently, the present study used two different doses. The first was an injection dose of 5.33 kBq/ml, as recommended by NEMA-2012, while the second was a low injection dose of 2.33 kBq/mL as a representative value for clinical application (approximately two hours after the first injection) for additional late PET/CT imaging (23). All phantom measurements were performed at 1/4 and 1/8 background/lesion (B/L) ratios. The CT scanning protocol (120 kVp tube-voltage, 100 mAs exposure) was used for CT-based attenuation correction.

In the study, each PET software was used to analyze the images. After reconstruction of the images for all PETs, analysis was performed according to section 7.4 of the NEMA NU2-2018 standard (24). For a quantitative assessment of image quality, the mean activity concentration (AC_{mean}) of each lesion was determined by using the mean standardized uptake value (SUV_{mean}). To achieve this, a circular region of interest (ROI) of the same diameter as a sphere was placed in the central slice of each sphere under CT imaging guidance as described by Kenta *et al.* (25). Therefore, all AC_{mean} values were obtained by plotting only one ROI passing through the centers of the lesions. In addition, to define the mean background AC for each image, five different ROIs with a size equal to the diameter of each lesion were drawn on different parts of the background.

By using the AC_{mean} values and the averages of 5 background AC_{mean} values for each lesion, the mean recovery coefficient (RC_{mean}) for each PET image was calculated following equation 1 provided in Srinivas *et al* study (26).

$$RC_{mean} = \frac{\text{Measured } AC_{mean} - \text{Background } AC_{mean}}{\text{Actual } AC_{mean} - \text{Actual Background } AC_{mean}} \quad (1)$$

Five independent observers (two nuclear medicine physicists and three nuclear medicine physicians) applied a visual score (VS) test to the PET images of the phantom. The group used the following criteria to provide visual scores: "1: Absolutely none; 2: May not be; 3: It may/may not be; 4: Maybe yes; 5: Definitely yes."

Statistical analysis

The Wilcoxon signed-rank test, a nonparametric statistical hypothesis test, was used to compare two

parameters, corresponding to the Analog PET-1, Analog PET-2, and digital PET systems, for RC_{mean} values. All parameters were analyzed using SPSS (version 29.0.2.0) and statistical significance was indicated by a p-value of less than 0.05.

RESULTS

Figure 2 shows the injection dose of 2.33 kBq/ml with an imaging duration of 1 min and a B/L=1/4 activity rate. No lesions were observed with analog PET-1, whereas 8 mm and 10 mm lesions were observed with analog PET-2 and dPET, respectively. When the injection dose was increased to 5.33 kBq/ml under the same conditions, lesions 8 mm and 10 mm in length were first observed in all 3 PET scans at the first minute.

	2.33 kBq /ml Injection Dose and B/L=1/4.		5.33 kBq /ml Injection Dose and B/L=1/4	
	1 min.	5 min.	1 min.	5 min.
analog PET-1				
analog PET-2				
digital PET				

Figure 2. Phantom PET images of fabricated sub-centimeter lesion for the injection doses of 2.33 kBq/ml and 5.33 kBq/ml with imaging durations of 1 and 5 minutes and B/L=1/4 activity rate for all three devices.

Figure 3 shows the injection dose at 2.33 kBq/ml with an imaging duration of 1 min, and B/L=1/8 shows 8 mm and 10 mm lesions in analog PET-1, 6 mm lesions in analog PET-2 and 6 mm, and 4 mm lesions in dPET. When the injection dose was increased to 5.33 kBq/ml under the same conditions, 5mm, 6mm, 8mm and 10mm lesions were observed in the first minute for analog PET-1 and all lesions in the first minute for analog PET-2 and dPET.

Figure 4 shows the original over-centimeter lesions for injection doses of 2.33 kBq/ml with imaging times of one and five minutes. An activity ratio of B/L=1/4; starting from 17 mm, 22 mm, 28 mm, and 37 mm lesions was observed in the first minute in analog PET-1, while all lesions were observed in analog PET-2 and dPET. Figure 4 shows the original over-centimeter lesions for injection doses of 5.33 kBq/ml with imaging times of one and five minutes, as well as an activity ratio of B/L=1/8 and all lesions in the first minute for analog PET-1, analog PET-2 and dPET.

Figure 5 shows the original lesions for injection doses of 2.33 kBq/ml and 5.33 kBq/ml with imaging times of 1 and 5 minutes, as well as an activity ratio

of B/L=1/8 and all lesions in the first minute for analog PET-1, analog PET-2 and dPET.

	2.33 kBq /ml Injection Dose and B/L=1/8.		5.33 kBq /ml Injection Dose and B/L=1/8	
	1 min.	5 min.	1 min.	5 min.
analog PET-1				
analog PET-2				
digital PET				

Figure 3. Phantom PET images of fabricated sub-centimeter lesions for the injection doses of 2.33 kBq/ml and 5.33 kBq/ml with imaging durations of 1 and 5 minutes and B/L=1/8 activity rate for all three devices.

	2.33 kBq /ml Injection Dose and B/L=1/4.		5.33 kBq /ml Injection Dose and B/L=1/4	
	1 min.	5 min.	1 min.	5 min.
analog PET-1				
analog PET-2				
digital PET				

Figure 4. Phantom PET images of original over-centimeter lesions for the injection doses of 2.33 kBq/ml and 5.33 kBq/ml with imaging durations of 1 and 5 minutes and B/L=1/4 activity rate for all three devices.

	2.33 kBq /ml Injection Dose and B/L=1/8.		5.33 kBq /ml Injection Dose and B/L=1/8	
	1 min.	5 min.	1 min.	5 min.
analog PET-1				
analog PET-2				
digital PET				

Figure 5. Phantom PET images of original over-centimeter lesions for the injection doses of 2.33 kBq/ml and 5.33 kBq/ml with imaging durations of 1 and 5 minutes and B/L=1/8 activity rate for all three devices.

Table 2 shows the RC_{mean} results at 1 min, 2 min, 3 min, and 5 min for sub-centimeter lesions with B/L values of 1/4 and 1/8 at 2.33 kBq/ml and 5.33 kBq/

ml activity for all three devices. According to table 2, there was no lesion in the first minute on the analog PET-1 device, while the RC_{mean} values of the 8 mm and 10 mm lesions were 0.15 and 0.24, respectively, starting from the second minute.

With respect to analog PET-2, the RC_{mean} values at 6 mm, 8 mm and 10 mm were 0.05, 0.3 and 0.39, respectively, by the third minute. Finally, on digital PET, the RC_{mean} values for the 6 mm, 8 mm and 10 mm long lesions were 0.1, 0.45, and 0.48, respectively, by the third minute. There was a significant difference between analog PET-1 and analog PET2, as well as between analog PET-1 and dPET (p<0.05). However, there was no significant difference between analog PET-2 and dPET (p>0.05).

Table 2. RC values at the 1st, 2nd, 3rd and 5th minutes of sub-centimeter lesions with 2.33 MBq and 5.33 MBq activities and B/L ratio of 1/4 and 1/8 for A1 (first Analog), A2 (second Analog) and D (Digital) PETs

Time	PET	B/L	2.33 MBq					5.33 MBq				
			4 mm	5 mm	6 mm	8 mm	10 mm	4 mm	5 mm	6 mm	8 mm	10 mm
1 min	A1	1/4	0.00	0.00	0.00	0.00	0.00	0.00	0.00	0.00	0.27	0.30
	A1	1/8	0.00	0.00	0.00	0.22	0.35	0.00	0.07	0.09	0.32	0.42
	A2	1/4	0.00	0.00	0.00	0.25	0.32	0.00	0.00	0.00	0.39	0.40
	A2	1/8	0.00	0.00	0.26	0.38	0.52	0.15	0.20	0.37	0.47	0.60
	D	1/4	0.00	0.00	0.00	0.35	0.41	0.00	0.00	0.00	0.47	0.50
	D	1/8	0.00	0.00	0.36	0.44	0.67	0.20	0.26	0.45	0.50	0.75
2 min	A1	1/4	0.00	0.00	0.00	0.15	0.24	0.00	0.00	0.00	0.32	0.34
	A1	1/8	0.00	0.00	0.22	0.32	0.36	0.00	0.15	0.30	0.39	0.45
	A2	1/4	0.00	0.00	0.00	0.28	0.36	0.00	0.00	0.00	0.41	0.45
	A2	1/8	0.00	0.15	0.32	0.43	0.55	0.20	0.25	0.40	0.51	0.63
	D	1/4	0.00	0.00	0.00	0.40	0.44	0.00	0.10	0.15	0.51	0.55
	D	1/8	0.00	0.27	0.43	0.55	0.71	0.28	0.32	0.52	0.66	0.80
3 min	A1	1/4	0.00	0.00	0.00	0.18	0.31	0.00	0.00	0.00	0.34	0.36
	A1	1/8	0.00	0.12	0.28	0.36	0.40	0.13	0.22	0.35	0.42	0.49
	A2	1/4	0.00	0.00	0.05	0.30	0.39	0.00	0.00	0.30	0.45	0.50
	A2	1/8	0.00	0.23	0.38	0.48	0.62	0.22	0.28	0.44	0.56	0.65
	D	1/4	0.00	0.00	0.10	0.45	0.48	0.00	0.15	0.35	0.55	0.60
	D	1/8	0.14	0.30	0.45	0.62	0.74	0.30	0.35	0.55	0.70	0.82
5 min	A1	1/4	0.00	0.00	0.00	0.22	0.35	0.00	0.00	0.20	0.36	0.40
	A1	1/8	0.00	0.19	0.25	0.38	0.44	0.15	0.24	0.38	0.45	0.52
	A2	1/4	0.00	0.00	0.10	0.37	0.44	0.15	0.15	0.32	0.47	0.53
	A2	1/8	0.00	0.25	0.42	0.50	0.59	0.26	0.30	0.46	0.58	0.69
	D	1/4	0.00	0.00	0.25	0.50	0.55	0.00	0.20	0.40	0.55	0.65
	D	1/8	0.30	0.34	0.50	0.63	0.75	0.32	0.37	0.58	0.72	0.84

Table 2 shows that for sub-centimeter lesions imaged at 1, 2, 3, and 5 minutes, an activity ratio of B/L=1/4, and injection doses of 5.33 kBq/ml, the RC_{mean} for the smallest lesion visible on analog PET-1, 6 mm, was 0.2 at 5 minute. For the same conditions, the RC_{mean} value for the smallest lesion of 5 mm on analog PET-2 was 0.15 at five minutes, while the RC_{mean} value on dPET was 0.2. There was a significant difference between analog PET-1 and analog PET-2 and between analog PET-1 and dPET (p<0.05). However, there was no significant difference between analog PET-2 and dPET (p>0.05).

In table 2, for sub-centimeter lesions, imaging times of 1 min, 2 min, 3 min, and 5 min were used, with an activity ratio of B/L=1/8 and injection doses of 2.33 kBq/ml. In analog PET-1, from minute 3 onward, the RC mean values for 5 mm, 6 mm, 8 mm, and 10 mm lesions were 0.12, 0.28, 0.36, and 0.4, respectively. In analog PET-2, from minute 3 onward, the RC mean values for 5 mm, 6 mm, 8 mm, and 10 mm lesions were 0.23, 0.38, 0.48 and, 0.62, respectively. On dPET, the smallest lesion (4 mm) was also visible at the third minute. The RC_{mean} values are 0.14, 0.3, 0.45, 0.62, and 0.74. There was a significant difference between analog PET-1 and analog PET-2, between analog PET-2 and dPET and between analog PET-1 and dPET (p<0.05).

Table 2 shows sub-centimeter lesions, with imaging times of 1 min, 2 min, 3 min, and 5 min, an activity ratio of B/L=1/8, and injection doses of 5.33 kBq/ml. In analog PET-1, the smallest lesion of 4 mm is visible from minute three onward. The RC_{mean} values were 0.13, 0.22, 0.35, 0.42, and 0.49. On analog PET-2 and dPET, all lesions were visible at minute one. The RC_{mean} values for analog PET-2 were 0.15, 0.2, 0.37, 0.47, and 0.6. For digital PET, the RC_{mean} values were 0.2, 0.26, 0.45, 0.5, and 0.75. There was a significant difference between the analog PET-1 and analog PET-2 analog, as well as between the PET-1 analog and dPET (p<0.05). However, there was no significant difference between the analog PET-2 and dPET (p>0.05).

In table 3, for over-centimeter lesions, imaging times of 1 min, 2 min, 3 min, and 5 min, an activity ratio of B/L=1/8 and injection doses of 5.33 kBq/ml were used. In analog PET-1, analog PET-2 and dPET, all lesions were visible by minute one. For analog PET -1, the RC_{mean} values of the 10 mm, 13 mm, 17 mm, 22 mm, 28 mm, and 37 mm lesions were 0.42, 0.43, 0.45, 0.47, 0.52, and 0.55, respectively. For analog PET-2, the RC_{mean} values for the 10 mm, 13 mm, 17 mm, 22 mm, 28 mm, and 37 mm lesions were 0.6, 0.63, 0.65, 0.7, 0.71, and 0.71, respectively. For dPET, the RC_{mean} values of the 10 mm, 13 mm, 17 mm, 22 mm, 28 mm, and 37 mm lesions were 0.75, 0.78, 0.8, 0.82, 0.84, and 0.88, respectively. There were significant differences between analog PET-1 and analog PET-2, between analog PET-2 and dPET, and between analog PET-1 and dPET (p<0.05).

(A-1=analog PET-1; A-2=analog PET-2; D=digital PET).

In figure 6, the visual scoring values are shown for modified sub-centimeter lesions, depicting 1 min and 5 min for sub-centimeter lesions with B/L values of 1/4 (figure 6a) and 1/8 (figure 6c) at 2.33 kBq/ml activity. The B/L values are 1/4 (figure 6b) and 1/8 (figure 6d) at 5.33 kBq/ml activity for all three devices. According to figure-6a, analog PET-1 shows 8 mm and 10 mm lesions at five minutes. On analog PET-2 and dPET, 8 mm and 10 mm lesions, respectively, were observed at one minute. In

figure-6b, the smallest visible lesion for analog PET-1 at five minutes was 6 mm, while analog PET-2 and dPET showed a lesion of 5 mm. In figure-6c, at 5

minutes, the smallest visible lesion for analog PET-1 and analog PET-2 was 5 mm, while dPET showed a lesion of 4 mm.

Table 3. RC values at the 1st, 2nd, 3rd and 5th minutes of over-centimeter lesions with 2.33 MBq and 5.33 MBq activities and B/L ratio of 1/4 and 1/8 for A1 (first Analog), A2 (second Analog) and D (Digital) PETs.

Time	PET	B/L	2.33 MBq						5.33 MBq					
			10 mm	13 mm	17 mm	22 mm	28 mm	37 mm	10 mm	13 mm	17 mm	22 mm	28 mm	37 mm
1 min	A1	1/4	0.00	0.00	0.15	0.35	0.40	0.45	0.30	0.35	0.40	0.45	0.50	0.55
	A1	1/8	0.35	0.41	0.42	0.45	0.49	0.52	0.42	0.43	0.45	0.47	0.52	0.55
	A2	1/4	0.32	0.35	0.40	0.45	0.55	0.60	0.40	0.50	0.55	0.60	0.70	0.78
	A2	1/8	0.52	0.59	0.60	0.65	0.68	0.70	0.60	0.63	0.65	0.70	0.71	0.71
	D	1/4	0.41	0.45	0.49	0.55	0.60	0.68	0.50	0.60	0.65	0.70	0.74	0.80
	D	1/8	0.67	0.68	0.70	0.72	0.74	0.75	0.75	0.78	0.80	0.82	0.84	0.88
2 min	A1	1/4	0.24	0.30	0.35	0.40	0.45	0.48	0.34	0.40	0.45	0.50	0.55	0.60
	A1	1/8	0.36	0.45	0.48	0.50	0.55	0.58	0.45	0.50	0.52	0.55	0.58	0.60
	A2	1/4	0.36	0.40	0.45	0.50	0.55	0.65	0.45	0.55	0.61	0.65	0.71	0.75
	A2	1/8	0.55	0.64	0.70	0.72	0.73	0.75	0.63	0.71	0.72	0.75	0.78	0.80
	D	1/4	0.44	0.50	0.52	0.60	0.70	0.78	0.55	0.66	0.70	0.76	0.80	0.85
	D	1/8	0.71	0.78	0.84	0.87	0.88	0.90	0.80	0.82	0.85	0.88	0.90	0.92
3 min	A1	1/4	0.31	0.35	0.40	0.45	0.50	0.60	0.36	0.40	0.45	0.50	0.55	0.65
	A1	1/8	0.40	0.50	0.60	0.62	0.67	0.70	0.49	0.55	0.63	0.66	0.69	0.72
	A2	1/4	0.39	0.45	0.50	0.55	0.60	0.75	0.50	0.55	0.60	0.65	0.70	0.79
	A2	1/8	0.62	0.72	0.78	0.80	0.85	0.88	0.65	0.75	0.84	0.86	0.88	0.90
	D	1/4	0.48	0.53	0.60	0.65	0.68	0.80	0.60	0.65	0.69	0.74	0.78	0.85
	D	1/8	0.74	0.82	0.88	0.90	0.91	0.92	0.82	0.84	0.88	0.92	0.94	0.95
5 min	A1	1/4	0.35	0.40	0.45	0.50	0.60	0.64	0.40	0.45	0.5	0.55	0.60	0.69
	A1	1/8	0.44	0.54	0.62	0.65	0.68	0.72	0.52	0.60	0.64	0.66	0.70	0.74
	A2	1/4	0.44	0.50	0.55	0.65	0.70	0.82	0.53	0.58	0.62	0.68	0.74	0.84
	A2	1/8	0.59	0.75	0.84	0.89	0.9	0.92	0.69	0.8	0.86	0.9	0.92	0.94
	D	1/4	0.55	0.62	0.7	0.8	0.85	0.9	0.65	0.7	0.75	0.84	0.89	0.92
	D	1/8	0.75	0.85	0.91	0.92	0.94	0.97	0.84	0.86	0.9	0.93	0.96	0.98

Table4. RC values at the 1st, 2nd, 3rd and 5th minutes of sub-centimeter lesions with 2.33 MBq and 5.33 MBq activities and B/L ratio of 1/4 and 1/8 for A1 (first Analog), A2 (second Analog) and D (Digital) PETs.

Time	PET	B/L	2.33 MBq					5.33 MBq					
			4 mm	5 mm	6 mm	8 mm	10 mm	4 mm	5 mm	6 mm	8 mm	10 mm	
1 min	A1	1/4	1.0	1.0	1.0	1.0	1.0	1.0	1.0	1.0	1.0	1.8	2.2
	A1	1/8	1.0	1.0	1.0	3.0	3.2	1.0	1.4	1.8	3.0	3.8	3.8
	A2	1/4	1.0	1.0	1.0	2.0	2.4	1.0	1.0	1.0	2.6	3.0	3.0
	A2	1/8	1.0	1.0	1.0	3.4	5.0	1.4	2.0	2.8	4.0	5.0	5.0
	D	1/4	1.0	1.8	2.2	4.4	5.0	1.0	1.0	1.0	3.6	3.8	3.8
	D	1/8	1.0	1.8	2.2	4.4	5.0	1.6	2.4	3.4	4.6	5.0	5.0
5 min	A1	1/4	1.0	1.0	1.0	2.2	2.4	1.0	1.0	1.4	3.2	3.4	3.4
	A1	1/8	1.0	1.4	1.6	2.4	3.4	1.0	1.4	1.8	3.0	3.8	3.8
	A2	1/4	1.0	1.4	1.8	3.4	3.4	1.0	1.8	1.8	4.2	4.4	4.4
	A2	1/8	1.0	1.8	2.4	3.8	5.0	1.6	2.0	3.0	4.2	5.0	5.0
	D	1/4	1.0	1.6	2.0	3.8	4.0	1.0	2.0	2.0	4.6	5.0	5.0
	D	1/8	1.4	2.0	3.0	4.6	5.0	1.8	2.4	3.6	4.8	5.0	5.0

Table5. RC values at the 1st, 2nd, 3rd and 5th minutes of over-centimeter lesions with 2.33 MBq and 5.33 MBq activities and B/L ratio of 1/4 and 1/8 for A1 (first Analog), A2 (second Analog) and D (Digital) PETs.

Time	PET	B/L	2.33 MBq						5.33 MBq					
			10 mm	13 mm	17 mm	22 mm	28 mm	37 mm	10 mm	13 mm	17 mm	22 mm	28 mm	37 mm
1 min	A1	1/4	1.0	3.0	3.6	5.0	5.0	5.0	2.2	3.6	5.0	5.0	5.0	5.0
	A1	1/8	3.2	3.6	4.0	5.0	5.0	5.0	3.8	4.4	5.0	5.0	5.0	5.0
	A2	1/4	2.4	3.6	4.0	5.0	5.0	5.0	3.0	4.0	5.0	5.0	5.0	5.0
	A2	1/8	5.0	5.0	5.0	5.0	5.0	5.0	5.0	5.0	5.0	5.0	5.0	5.0
	D	1/4	3.4	4.4	4.4	5.0	5.0	5.0	4.0	5.0	5.0	5.0	5.0	5.0
	D	1/8	5.0	5.0	5.0	5.0	5.0	5.0	5.0	5.0	5.0	5.0	5.0	5.0
5 min	A1	1/4	2.4	4.0	5.0	5.0	5.0	5.0	3.4	4.0	5.0	5.0	5.0	5.0
	A1	1/8	3.4	4.0	5.0	5.0	5.0	5.0	3.8	4.4	5.0	5.0	5.0	5.0
	A2	1/4	3.4	4.4	5.0	5.0	5.0	5.0	4.4	4.6	5.0	5.0	5.0	5.0
	A2	1/8	5.0	5.0	5.0	5.0	5.0	5.0	5.0	5.0	5.0	5.0	5.0	5.0
	D	1/4	4.0	5.0	5.0	5.0	5.0	5.0	5.0	5.0	5.0	5.0	5.0	5.0
	D	1/8	5.0	5.0	5.0	5.0	5.0	5.0	5.0	5.0	5.0	5.0	5.0	5.0

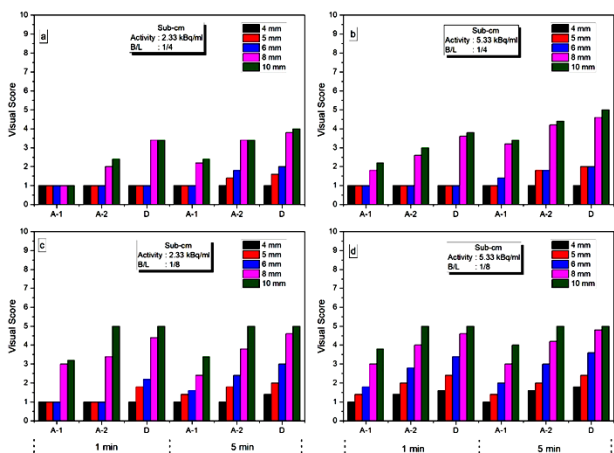


Figure 6. Visual scores of sub-centimeter lesions (4–10 mm) acquired with analog PET-1, analog PET-2, and digital PET under different activity and B/L conditions.

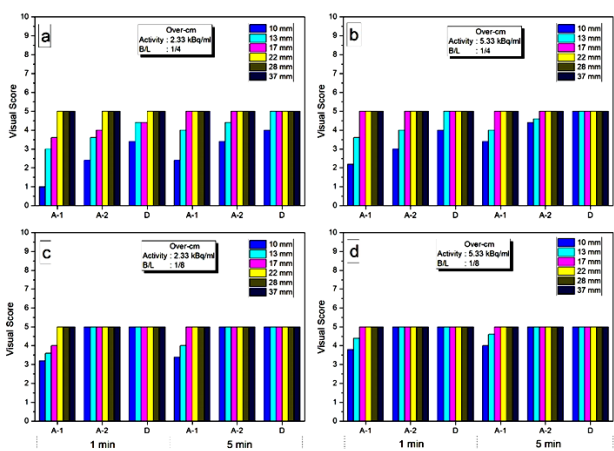


Figure 7. Visual scores of over-centimeter lesions (10–37 mm) acquired with analog PET-1, analog PET-2, and digital PET under different activity and B/L conditions.

As shown in figure-6d, the smallest visible lesion for analog PET-1 was 5 mm at one minute, while analog PET-2 and digital PET showed a lesion of 4 mm at the same time.

Figure 7 shows the visual scoring values for one min and five min for modified over-centimeter lesions. For those exceeding over-centimeter lesions, the B/L values were 1/4 (figure 7a) and 1/8 (figure 7c) at 2.33 kBq/ml activity. For all three devices, the B/L values were 1/4 (figure 7b) and 1/8 (figure 7d) at 5.33 kBq/ml activity. According to figure-7a, analog PET-1 shows a lesion of 10 mm at minute one for analog PET-2 and dPET, while the smallest visible lesion is 10 mm for analog PET-1 at minute 5. Figure 7b-d depict the smallest lesion (10 mm) among all three PET devices from minute one onward.

(1: Absolutely none; 2: May not be; 3: It may/may not be; 4: Maybe yes, 5: Definitely yes).

DISCUSSION

Advances in PET technology aim to increase the imaging quality of lesions. The dPET recently introduced into clinical practice is one of the most

important methods for accessing these lesions like small tumors. This new technology replaces PMT with SiPM, limiting the advancement in the technology only with the photon multiplication system. Besides, the analog PET technology is also widely employed in the clinic. It is unlikely that this technology will be abandoned soon. Thus, if a clinic operates on more than one PET with different brands or technologies (digital or analog), it is reasonable to consider them coequals only if they show identical performance.

A new generation of dPET devices contains SiPMs instead of PMTs, as used in analog PETs. This allows for a detector design with smaller crystals, better time, and spatial resolution. DPETs have the potential to improve the quality of images when compared to analog pets. In a study comparing the full width at half maximum (FWHM) of a GE analog and GE digital PETs, FWHMs were measured at 4.52 mm via GE Discovery MI PET with PMT and at 3.91 mm via Discovery GE PET/CT 710 PET with SiPM. There was an improvement of up to 16% in FWHMs with SiPM technology (18).

FWHM is very important in PET systems in terms of spatial resolution. SiPM technologies show a significant advantage in this respect. Many studies compared the FWHM between analog PET and digital PET, the measured FWHM was 4.4 mm for the former and 4.16 mm FWHM for the latter. In this context, an improvement of up to 6% in the FWHM was achieved thanks to SiPM technology (27, 28). There is limited research in the literature on phantom comparing analog-digital PET image quality for sub-centimeter lesions. In one of the studies on sub-centimeter lesion imaging, the effects of beta factors (between beta=50 and beta=400) were examined using the Q-Clear algorithm only for digital Discovery MI PET (25). The authors reported that the ideal beta value for optimal imaging of sub-centimeter lesions is 200. Similarly, the clinical beta value of our study was set to 200, and the RC_{mean} values determined by our study are quite similar to the RC_{mean} values of the mentioned study. The authors reported an RC_{mean} of 0.80 for a lesion of 10 mm, 0.50 for a lesion of 6 mm, and 0.30 for a lesion of 4 mm at an injection dose of 5.3 kBq/ml when the B/L was 1/8. However, our study reported an RC_{mean} of 0.84 for a lesion of 10 mm, 0.56 for a lesion of 6 mm, and 0.32 for a lesion of 4 mm. Our analysis assessed the image quality of sub-centimeter lesions in accordance with the NEMA-2012 (23). NEMA-2018 reports by comparing the results of three separate PETs with those of different brands and technologies (23, 24). In our study, there was no significant difference between dPET and the analog PET-2 in terms of performance. However, the analog PET-1 performed significantly worse than the former. Jenny Oddstig *et al.* compared the image quality of lesions greater than 1 cm (10 mm, 13 mm, 17 mm, 22 mm, 28 mm, and 37 mm diameter) in their

GE dPET and Philips Analog Gemini TOF PET phantom studies⁽²⁹⁾. They reported that while GE dPET gave an RC value exceeding 0.90 in a 17 mm diameter lesion, a lesion exceeding 0.90 RC for Philips Analog Gemini TOF PET was only a 37 mm diameter lesion. They also reported that GE dPET provided RC values 35% better than Philips Analog Gemini TOF PET (the RC values in their study were reported as $RC(17\text{ mm}) = 0.95$ for GE dPET and $RC(17\text{ mm}) = 0.65$ for Philips Gemini TOF PET). However, this study did not cover any analysis of sub-centimeter lesions. Our study analyzing sub-centimeter lesions revealed approximately 30% better RC values for digital PET than for analog PET-1 (table 3)⁽²⁹⁾. In another study comparing image quality, Rausch et al. assessed the image quality of lesions on a Siemens analog PET⁽³⁰⁾. Although they studied the image quality of lesions above 1 cm (10, 13, 17, 22, 28, and 37 mm in diameter), no information on the image quality of sub-centimeter lesions was reported. The authors reported that the RC values measured by the OSEM+PSF+TOF algorithm for lesions above 1 cm $RC(10\text{ mm}) = 0.285$ for $B/L=1/4$ and $RC(10\text{ mm}) = 0.424$ for $B/L=1/8$ were lower than the RC values ($RC(10\text{ mm}) = 0.516$ for $B/L = 1/4$ and $RC(10\text{ mm}) = 0.645$ $B/L = 1/8$) in the study of Jakoby et al.⁽³¹⁾. A comparison of our RC values for analog PET-2 (for $B/L= 1/4$ and $RC(10\text{ mm})$ was 0.530 (table 3), while for $B/L=1/8$ and for $RC(10\text{ mm})$ was 0.69 (table 3). Jakoby et al. reported these values as 0.516 for $B/L=1/4$ and $RC(10\text{ mm})$ and for 0.645 for $B/L=1/8$ and $RC(10\text{ mm})$ for the same reconstruction parameters (200×200matrix value, 2 iterations, 21 subsets), showing that these two analyses yielded similar results⁽³¹⁾.

Considering their technologies, there are significant differences between the RC_{mean} values of all three PET devices. Our study revealed approximately 15% greater RC_{mean} values for dPET with SiPM technology compared to the analog PET-2 with PMT technology. However, analog PET-1 exhibited a significant lack of performance, especially when compared to analog PET-2 and dPET. The analog PET-1 provides up to a 30% lower RC_{mean} compared to dPET.

In regard to the numerical relationship between the RC_{mean} and VS of lesions, as shown in the RC_{mean} graphs and VS graphs in the present study, for a lesion to achieve $VS=3$, $VS=4$, or $VS=5$, the RC_{mean} value must be at least 0.35, 0.45 or 0.60, respectively. Miwa et al. obtained a visual score close to five for a 10 mm lesion with a background of 5.3 kBq/mL and a beta of 200 at two minutes. In our study, the same beta value for the 10 mm lesion and visual score at one minute at $B/L 1/4$ was 3.8⁽²⁵⁾.

CONCLUSION

Although dPET, the first generation of dPETs

analyzed in the present study, yields relatively better RC_{mean} values than analog PETs, it cannot entirely eliminate the unfavorable impacts of PVE for sub-centimeter lesions. It appears that analog technology has improved remarkably, being used for many years. Therefore, when these devices are used interchangeably for additional late imaging or posttreatment imaging, it is necessary to consider the differences between the lesion imaging performances of PETs for accurate diagnosis. Furthermore, it should be noted that the dPET data analyzed in this study are from the first generation and show promising potential for improvement in the future. Soon after delivery, sub-centimeter lesions can be screened for RC values via dPET. An important milestone has been achieved by screening for early diagnosis.

ACKNOWLEDGEMENT

We would like to thank the members of the Nuclear Medicine Department of the Medipol Mega University Hospital and Prof. Dr. Cemil Taşçioğlu City Hospital.

Funding: None.

Ethical approval: Ethical approval was not required.

Conflicts of interest: The authors declare that they have no competing interests.

Author contributions statement: M.C.K and M.Ç wrote the main manuscript and prepared the figures. M.Ç conducted statistical analysis, while M.C.K prepared the tables. All authors reviewed and approved the manuscript.

REFERENCES

- Jiang W, Chalich Y, Deen MJ (2019) Sensors for positron emission tomography applications. *Sensors*, **19**(22): 1-53.
- Roncali E and Cherry SR (2011) Application of silicon photomultipliers to positron emission tomography. *Ann Biomed Eng*, **39**(4): 1358-77.
- Sun F, Duan N, Lo G-Q (2013) Highly efficient silicon photomultiplier for positron emission tomography application. *Int. Jou. of Biomed. and Bio. Eng.* **7**(9): 555-557.
- del Sordo S, Abbene L, Caroli E, Mancini AM, Zappettini A, Ubertini P (2009) Progress in the development of CdTe and CdZnTe semiconductor radiation detectors for astrophysical and medical applications. *Sensors*, **9**: 3491-526.
- Komarov S, Yin Y, Wu H, Wen J, Krawczynski H, Meng LJ, et al. (2012) Investigation of the limitations of the highly pixilated CdZnTe detector for PET applications. *Phys Med Biol*, **57**(22): 7355-80.
- Ariño-Estrada G, Mitchell GS, Kwon S II, Du J, Kim H, Cirignano LJ, et al. (2018) Towards time-of-flight PET with a semiconductor detector. *Phys Med Biol*, **63**(4): 1-9.
- Soret M, Bacharach SL, Buvat I (2007) Partial-volume effect in PET tumor imaging. *Journal of Nuclear Medicine*, **48**: 932-45.
- Hudson HM and Larkin RS (1994) Accelerated Image reconstruction using ordered subsets of projection data. *IEEE Transactions on Medical Imaging*, **13**: 601-609.
- Daube-Witherspoon ME, Surti S, Perkins AE, Karp JS (2014) Determination of accuracy and precision of lesion uptake measurements in human subjects with time-of-flight pet. *Journal of Nuclear Medicine*, **55**(4): 602-7.
- Belleve D, Blanc Fournier C, Switsers O, Dugué AE, Levy C, Allouache D, et al. (2014) Staging the axilla in breast cancer patients with 18F-FDG PET: How small are the metastases that we can detect with new generation clinical PET systems? *Eur J Nucl*

- Med Mol Imaging*, **41**(6): 1103–12.
11. Ahn S, Ross SG, Asma E, Miao J, Jin X, Cheng L, et al. (2015) Quantitative comparison of OSEM and penalized likelihood image reconstruction using relative difference penalties for clinical PET. *Phys Med Biol*, **60**(15): 5733–51.
 12. Ross S. Q.Clear: A Bayesian penalized likelihood reconstruction algorithm for PET image quantitation. *GE Healthcare*; 2014. *DOC1474189 Rev 3*: 1-9.
 13. Assing MA, Patel BK, Karamsadkar N, Weinfurter J, Usmani O, Kiluk JV, et al. (2017) A comparison of the diagnostic accuracy of magnetic resonance imaging to axillary ultrasound in the detection of axillary nodal metastases in newly diagnosed breast cancer. *Breast Journal*, **23**(6): 647–55.
 14. Aktaş A, Gürleyik MG, Aksu SA, Aker F, Güngör S (2022) Diagnostic value of axillary ultrasound, MRI, and 18F-FDG-PET/CT in determining axillary lymph node status in breast cancer patients. *Eur J Breast Health*, **18**(1): 37–47.
 15. Morawitz J, Bruckmann NM, Dietzel F, Ullrich T, Bittner AK, Hoffmann O, et al. (2022) Comparison of nodal staging between CT, MRI, and [18F]-FDG PET/MRI in patients with newly diagnosed breast cancer. *Eur J Nucl Med Mol Imaging*, **49**(3): 992–1001.
 16. Xu C, Garutti E, Mandai S, Charbon E (2013) Comparison of digital and analog silicon photomultiplier for positron emission tomography application. *EJNMMI Phys*, **9**(1):3: 1-7.
 17. Recker MC, Cazalas EJ, McClory JW, Bevins JE (2019) Comparison of SiPM and PMT performance using a Cs₂LiYCl₆:Ce³⁺ (CLYC) scintillator with two optical windows. *IEEE Trans Nucl Sci*, **66**(8): 1959-65.
 18. Wagatsuma K, Miwa K, Sakata M, Oda K, Ono H, Kameyama M, et al. (2017) Comparison between new-generation SiPM-based and conventional PMT-based TOF-PET/CT. *Physica Medica*, **42**: 203–10.
 19. Tsutsui Y, Awamoto S, Himuro K, Kato T, Baba S, Sasaki M (2020) Evaluating and comparing the image quality and quantification accuracy of SiPM-PET/CT and PMT-PET/CT. *Ann Nucl Med*, **34**(10): 725–35.
 20. Adler S, Seidel J, Choyce P, Knopp M V., Binzel K, Zhang J, et al. (2017) Minimum lesion detectability as a measure of PET system performance. *EJNMMI Phys*, **4**(1): 1-14.
 21. Karlberg AM, Sæther O, Eikenes L, Goa PE (2016) Quantitative comparison of PET performance—siemens biograph mCT and mMR. *EJNMMI Phys*, **3**(1): 1-14.
 22. Hsu DFC, Ilan E, Peterson WT, Uribe J, Lubberink M, Levin CS (2017) Studies of a next-generation silicon-photomultiplier-based time-of-flight PET/CT system. *Journal of Nuclear Medicine*, **58**(9): 1511–8.
 23. NEMA NU 2-2012 (2013) Performance measurements of positron emission tomographs [Internet]. Available from: www.medicalimaging.org/
 24. NEMA Standards Publication NU 2-2018 (2018) Performance Measurements of Positron Emission Tomographs (PETS) [Internet]. Available from: www.nema.org
 25. Miwa K, Wagatsuma K, Nemoto R, Masubuchi M, Kamitaka Y, Yamao T, et al. (2020) Detection of sub-centimeter lesions using digital TOF-PET/CT system combined with Bayesian penalized likelihood reconstruction algorithm. *Ann Nucl Med*, **34**(10): 762–71.
 26. Srinivas SM, Dhurairaj T, Basu S, Bural G, Surti S, Alavi A (2009) A recovery coefficient method for partial volume correction of PET images. *Ann Nucl Med*, **23**(4): 341–8.
 27. López-Mora DA, Carrió I, Flotats A (2022) digital PET vs analog PET: Clinical Implications? *Seminars in Nuclear Medicine*, **52**: 302-311.
 28. Fuentes-Ocampo F, López-Mora DA, Flotats A, Paillahueque G, Camacho V, Duch J, et al. (2019) Digital vs. analog PET/CT: intra-subject comparison of the SUVmax in target lesions and reference regions. *Eur J Nucl Med Mol Imaging*, **46**(8): 1745-1750.
 29. Oddstig J, Leide Svegborn S, Almquist H, Bitzén U, Garpered S, Hedeer F, et al. (2019) Comparison of conventional and Si-photomultiplier-based PET systems for image quality and diagnostic performance. *BMC Med Imaging*, **19**(1): 1-9.
 30. Rausch I, Cal-González J, Dapra D, Gallowitsch HJ, Lind P, Beyer T, et al. (2015) Performance evaluation of the Biograph mCT Flow PET/CT system according to the NEMA NU2-2012 standard. *EJNMMI Phys*, **2**(1): 1–17.
 31. Jakoby BW, Bercier Y, Conti M, Casey ME, Bendriem B, Townsend DW (2011) Physical and clinical performance of the mCT time-of-flight PET/CT scanner. *Phys Med Biol*, **56**(8): 2375–89.

